Electronic Supplementary Material (ESI) for Chemical Communications.
This journal is © The Royal Society of Chemistry 2020

A Novel Water-Soluble Quinoline-Indole Derivative as Three-Photon Fluorescent Probe for Identifying Nucleolus RNA and Mitochondrial DNA

Imad Elddin Haj Elhussin[¶a], Sijing Zhang[¶a], Jiejie Liu[¶b], Dandan Li[c] Qiong Zhang[a]*, Shengli Li[a], Xiaohe Tian[b], Jieying Wu[a], Yupeng Tian[a]*

[a] *Department of Chemistry, Key Laboratory of Functional Inorganic Material Chemistry of Anhui Province, Anhui University, Hefei 230601, P. R. China*

[b] *School of Life Science, Anhui University, Hefei 230039, P. R. China*

[c] *Institutes of Physics Science and Information Technology, Anhui University, Hefei 230039, P. R. China*

¶ These authors contributed equally to this work.

E-mail address: zhangqiong.314@163.com yptian@ahu.edu.cn

Materials and apparatus

All chemicals were purchased as reagent grade and used without further purification. The solvents were dried and distilled according to standard procedures. IR spectra (4000 - 400 cm^{-1}), as KBr pellets, were recorded on a Nicolet FT-IR 870 SX spectrophotometer. ^{1}H-NMR spectra were performed on a Bruker 400 Hz Ultra shield spectrometer and reported as parts per million (ppm) from TMS (δ), ^{13}C-NMR spectra were obtained on a Bruker Advance 100 MHz NMR spectrometer. UV-*vis* absorption spectra were recorded on a UV-265 spectrophotometer. Fluorescence measurements were carried out on a Hitachi F-7000 fluorescence spectrophotometer.

Experimental Section

1.1 Synthesis and characterization

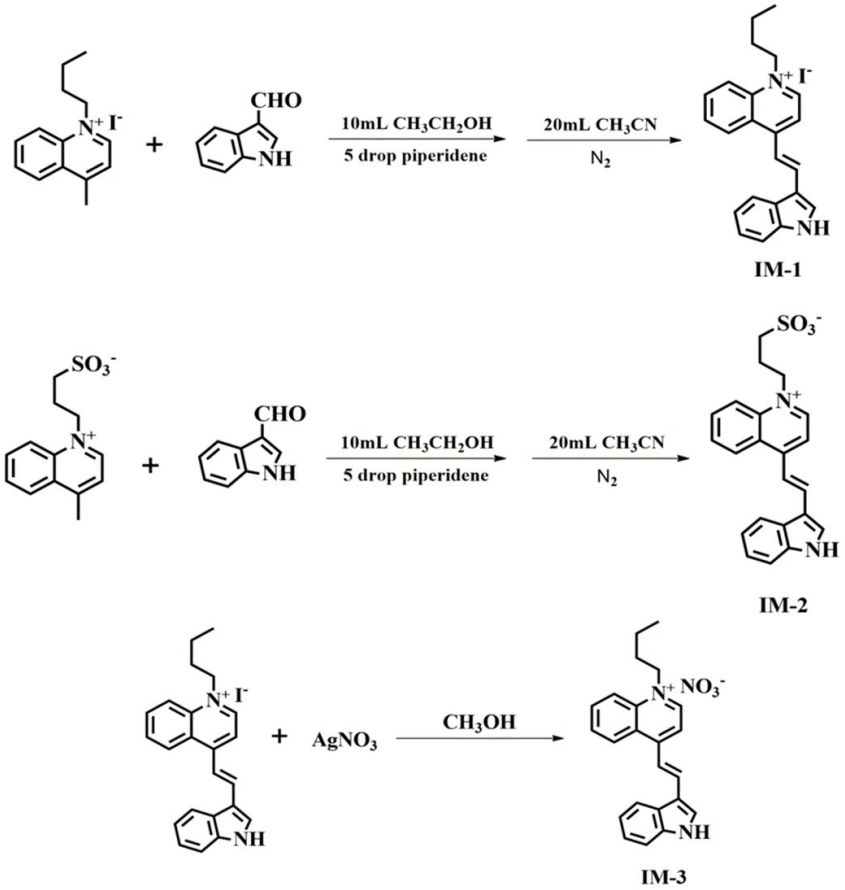

Figure. S1. Synthetic routes of **IM-1** to **IM-3**.

IM-1: By using a 100 mL three-necked flask fitted with a stirrer and a condenser, in N_2 atmosphere, the 1H-indole-3-carbaldehyde (0.4 mmol), 1-butyl-4-methylquinolin -1-ium iodide (0.4 mmol) was dissolved in 20 mL acetonitrile and 10 mL ethanol. Five

drops of piperidine were added to the mixture. Then the solution was heated to reflux for 4 h. The compound was gotten by filtration wash with acetonitrile. Red powder was obtained by drying in vacuum. ESI-m/z [M] $C_{23}H_{23}N_2I$ calcd: 327.19 (M) found: 327.19 (M). ^{1}H NMR (400 MHz, DMSO-d_6) δ 12.18 (s, 1H), 9.16 (d, J = 6.7 Hz, 1H), 8.99 (d, J = 8.5 Hz, 1H), 8.60 (d, J = 15.5 Hz, 1H), 8.50 – 8.39 (m, 1H), 8.36 (s, 1H), 8.22 (dd, J = 20.2, 12.6 Hz, 1H), 8.10 – 7.93 (m, 1H), 7.54 (d, J = 4.9 Hz, 1H), 7.40 – 7.20 (m, 1H), 4.88 (t, J = 7.3 Hz, 2H), 3.34 (s, 2H), 2.50 (d, J = 1.2 Hz, 2H), 2.13 – 1.70 (m, 2H), 1.42 (dd, J = 15.0, 7.6 Hz, 2H), 0.95 (t, J = 7.3 Hz, 3H). ^{13}C NMR (100 MHz, DMSO-d_6) δ 153.77, 145.98, 138.81, 137.84, 137.38, 134.71, 132.92, 128.47, 126.53, 125.75, 125.43, 123.12, 121.50, 120.30, 118.86, 114.62, 113.55, 112.72, 112.67, 55.63, 31.23, 19.20, 13.46. IR (KBr, cm^{-1}) selected bands: 3093, 2932, 2359, 1562, 1392, 1221, 1123, 855, 756.

IM-2: By using a 100 mL three-necked flask fitted with a stirrer and a condenser, in N_2 atmosphere, the 1H-indole-3-carbaldehyde (0.4 mmol),3-(4-methylquinolin-1-ium -1-yl)propane-1-sulfonate (0.4 mmol), 20 mL of acetonitrile and 10 mL ethanol were mixed. Five drops of piperidine were added to the mixture. Then the solution was heated to reflux for 4 h. The compound was gotten by filtration wash with acetonitrile. Red powder was obtained by drying in vacuum. ESI-m/z [M] $C_{22}H_{20}N_2O_3S$ calcd: 393.12 (M), found: 393.12 (M). ^{1}H NMR (400 MHz, DMSO-d_6) δ 12.16 (s, 1H), 9.15 (d, J = 6.5 Hz, 1H), 8.97 (d, J = 8.3 Hz, 1H), 8.60 (s, 1H), 8.58 – 8.54 (m, 1H), 8.43 (d, J = 6.6 Hz, 1H), 8.34 (s, 1H), 8.26 (s, 1H), 8.20 (t, J = 8.0 Hz, 1H), 8.05 (s, 1H), 8.01 (d, J = 7.0 Hz, 1H), 7.97 (d, J = 7.5 Hz, 1H), 7.53 (s, 1H), 7.29 (s, 1H), 5.03 (s, 2H), 2.57 (t, J = 6.7 Hz, 2H), 2.26 (d, J = 7.2 Hz, 2H). ^{13}C NMR (100 MHz, DMSO-d_6) δ 154.29, 146.69, 139.18, 138.40, 137.87, 135.24, 133.33, 128.96, 126.98, 126.30, 125.92, 123.60, 121.99, 120.80, 119.35, 115.11, 114.12, 113.32, 113.14, 55.26, 47.95, 26.30. IR (KBr, cm^{-1}) selected bands: 3447, 3201, 2357, 1575, 1412, 1203, 1039, 749, 603.

IM-3: The (E)-4-(2-(1H-indol-3-yl)vinyl)-1-butylquinolin-1-ium iodide (0.4 mmol) and silver nitrate (0.4 mmol) in methanol was added in a 100 mL flask fitted with a stirrer and a condenser. Then the solution was heated at 70 ℃ for 2 h in dark. black

solution was gotten after filtration. Finally, the red powder was obtained by evaporating. ESI-m/z [M] $C_{23}H_{23}N_3O_3$ calcd: 327.19 (M), found: 327.19 (M). ^{1}H NMR (400 MHz, DMSO-d_6) δ 12.21 (s, 1H), 9.15 (d, J = 6.7 Hz, 1H), 8.97 (d, J = 8.5 Hz, 1H), 8.59 (d, J = 15.6 Hz, 1H), 8.49 – 8.40 (m, 2H), 8.35 (d, J = 2.9 Hz, 1H), 8.24 (ddd, J = 25.1, 10.7, 5.4 Hz, 2H), 8.00 (dd, J = 21.6, 11.8 Hz, 2H), 7.61 – 7.49 (m, 1H), 7.37 – 7.24 (m, 2H), 4.87 (t, J = 7.4 Hz, 2H), 2.01 – 1.82 (m, 2H), 1.52 – 1.32 (m, 2H), 0.95 (t, J = 7.4 Hz, 3H). ^{13}C NMR (100 MHz, DMSO-d_6) δ 154.29, 146.49, 139.32, 138.35, 137.90, 135.23, 133.43, 128.98, 127.02, 126.26, 125.93, 123.64, 122.01, 120.79, 119.35, 115.13, 114.05, 113.23, 113.18, 56.14, 31.73, 19.70, 13.96.

1.2 Crystallography

The single crystals of **IM-1** and **IM-2**, suitable for X-ray diffraction analysis, were obtained from methanol solution at room temperature. The relevant crystal data and structural parameters were summarized in Table S1. The selected bond distances and angles were listed in Table S2.

The X-ray diffraction measurements were accomplished on a Bruker SMART CCD area detector using graphite monochromated Mo-Kα radiation (λ = 0.71069 Å) at 298(2) K. Intensity data were collected in the variable ω-scan mode. The structures were solved by direct methods and difference Fourier transformations. The nonhydrogen atoms were refined anisotropically and hydrogen atoms were introduced geometrically. Calculations were performed with SHELXTL-97 program package. The conjugation extent of IM-1 and IM-2 were similar. The bond length of C(6)-C(7) is 1.440Å, C(2)=C(6) is 1.350 Å and C(2)-C(11) is 1.431 Å, which suggested that the quinoline-indole derivatives possess a highly π-electron delocalized system.

1.3 Computational details

The ground states for each molecule were calculated using the density functional theory level with the B3LYP functional employing a 6-31G* basis set. The absorption energies were investigated by time-dependent density functional theory (TD-DFT). All calculations were performed by the use of the Gaussian 03 suite of programs.

1.4 Three-photon excitation fluorescence (3PEF) measurements

All the samples were contained in 1cm-optical length quartz liquid cell and

Rhodamin 6G as the standard sample for intensity comparison. Spectrometer: Ocean Optics QE65 Pro (300-2500 nm). Laser: Coherent Astrella+TOPAS Prime (1100-1800) nm, 1 kHz, 120 fs. All the results provided here are the 10 times average results[1-2].

Theory:

$$\sigma_{3s=}\frac{c_R \times n_s \times f_s \times Q_R}{c_s \times n_R \times f_R \times Q_S} \times \sigma_{3R}$$

where the subscripts "s" and "r" represent sample and reference (here, Rhodamine 6G in ethanol solution at a concentration of 1.0×10^{-3} mol/L was used as reference), respectively. F is the overall fluorescence collection efficiency intensity of the fluorescence signal collected by the fiber spectra meter. Q, *n* and *c* are the quantum yield of the fluorescence, the refractive index of solvent, and the concentration of the solution, respectively.

1.5 UV-vis spectra and Fluorescence titration of IM-3 with DNA/RNA

The sequence of DNA (CAS: 73049-39-5). It was purchased from ThermoFisher Ltd. Co. ORIGIN. EcoRI site.

```
   1 aattcaggat gcctcttgtg ttggcctagg caagtccaat cttccactcg agttgcgaag
  61 gaaagctggg cattgctctc gagtgactgc agggccaata gacgtcatct aggcttgtgt
 121 ccagaagcca atgttcctct ccaggggcga cagggatctc ggggttgcat tccagacgca
 181 cccggggaga caggcattca tctcgagtgg aagcaaagaa ccccgctctg ctctcgaatc
 241 gcgacgggta tctcttggag ctcactgggt ggactcaagg gagtcaagcc tcctgaggcg
 301 tttggagaga ggccgcgaga ttggtctcta ggccatgcag gagacgaagg ccctcactct
 361 cgataacggc ggaatctcgg ggttgttctc gagcggcggc cccagtgtgc ggtttctcac
 421 gaggtacgac ggcgaggtca gtgagcctct cgtggggcgc cagggaagtc gggtctccat
 481 gcgagtggcg agggggagcg cgtcattgct cgcgagccat gggaggggac tctggcctcg
 541 agacgtgttg aagaaggtct ctcgaggtct ttcccgggtt gaggcaggaa accctgggtt
 601 ccctcgactt gtgcaggtga cctcagggga cttctcatgg tggctctgcg aagccaggga
 661 aactggaggt gggaggggcc tctcgggact ccactgggtt tggtgcattg gaagagggcc
```

RNA (CAS:63231-63-0) was purchased from Sigma-Aldrich Ltd. Co. UV-vis absorption spectra were recorded on a UV-265 spectrophotometer. Fluorescence measurements were carried out on a Hitachi F-7000 fluorescence spectrophotometer.

The absorption bands of IM-3 at 287 nm and 473 nm displayed clear hypochromicity with hypochromism H % (H % = 100(Afree-Abound)/Afree) upon adding an increasing concentration of DNA. The bands at 282-nm and 481-nm were equal to 24.3 % and 47.1 %, respectively.

1.6 Molecular docking with DNA/RNA

The crystal structure of RNA（ID:5TDK, CCGGCGCCGG/CCGGCGCCGG）were retrieved from PDB database[3]. Explicit hydrogen atoms were added, and all water molecules were then deleted. The structure of RNA were processed. The active-site cavities of RNA is defined using the biggest cavity of the surface of RNA. Docking was carried out using the docking method of CDOCK vina software (version 2016, The Biovia Co.)[4]. The parameter was set as default.

The distribution of HOMO and LUMO of IM-3 indicated that the quinoline group was prone to combine with DNA/RNA.

1.7 ^{1}H NMR titration experiments.

^{1}H NMR titration experiments of **IM-3** with NA were performed in DMSO-d_6/D_2O (v/v, 1:1) at room temperature. To five stock solutions of **IM-**3 (500 μL, 1 mM), 10 μM, 20 μM, 30 μM, 40 μM of stock solutions containing DNA/RNA were in sample, respectively.

STD-NMR was performed on a 700 MHz Bruker spectrometer equipped with a triple resonance cryoprobe.

The docking results (Fig.S 25) indicated that IM-3 obtained a positive charge and lipophilicity. IM-3 could interact with DNA/RNA through weak forces or secondary bond interactions easily.

1.8 Cell imaging

HepG2 cells were purchasing from Cell Resource Center, Shanghai Institutes for Biological Sciences, Chinese Academy of Science (www.cellbank.org.cn.). Resource number: 3131C0001000700072. HepG2 cells were seeded in 24-well glass bottom plate at a density of 2 × 104 cells per well and grown for 96 h. For live cell imaging, cell cultures were incubated with the complexes (10% PBS: 90% cell media) at concentration 10 μM and maintained at 37 °C in an atmosphere of 5% CO_2 and 95% air for incubation times ranging for 30 min. The cells were then washed with PBS (3 × 1 mL per well) and 1 mL of PBS was added to each well. The cells were imaged using confocal laser scanning microscopy using oil immersion lenses.

Owing to the excellent bio-compability and 3PA activities of IM-3 in vitro, the

intracellular distribution and photo-physical properties in cells were investigated to explore the biological application. Firstly, the cell viability data for HepG2 cells (human liver carcinoma cells, purchasing from Cell Resource Center, Shanghai Institutes for Biological Sciences, Chinese Academy of Sciences) treated with IM-3 was shown in MTT assay (Fig.S 26). The results indicated a negligible toxicity of IM-3, and speculated at the potential for intracellular imaging.

1.9 STED imaging

STED nanoscopy experiments were performed under a Leica DMi8 confocal microscope equipped with a Leica TCS SP8 STED-ONE unit, the compound was excited under an STED laser, and the emission signals were collected using HyD reflected light detectors. Specimen living cells were prepared using a method similar to normal confocal microscopy described previously. The STED micrographs were further processed using "deconvolution wizard" function using Huygens Professional software (version: 16.05) under authorized license.

STED microscopy of IM-3 was performed without applying 3PF. In STED nanoscopy imaging, two excitation laser beams are adopted. One laser beam is the excitation beam, which was used for exciting IM-3 to the excited state (592 nm), and the other is the STED beam, which was modulated to a "donut" shape and was concentric with the excitation beam (590-600nm). In this case, the STED beam depleted the emission of the excited florescence probe by generating stimulated emission with the same wavelength as the STED beam.

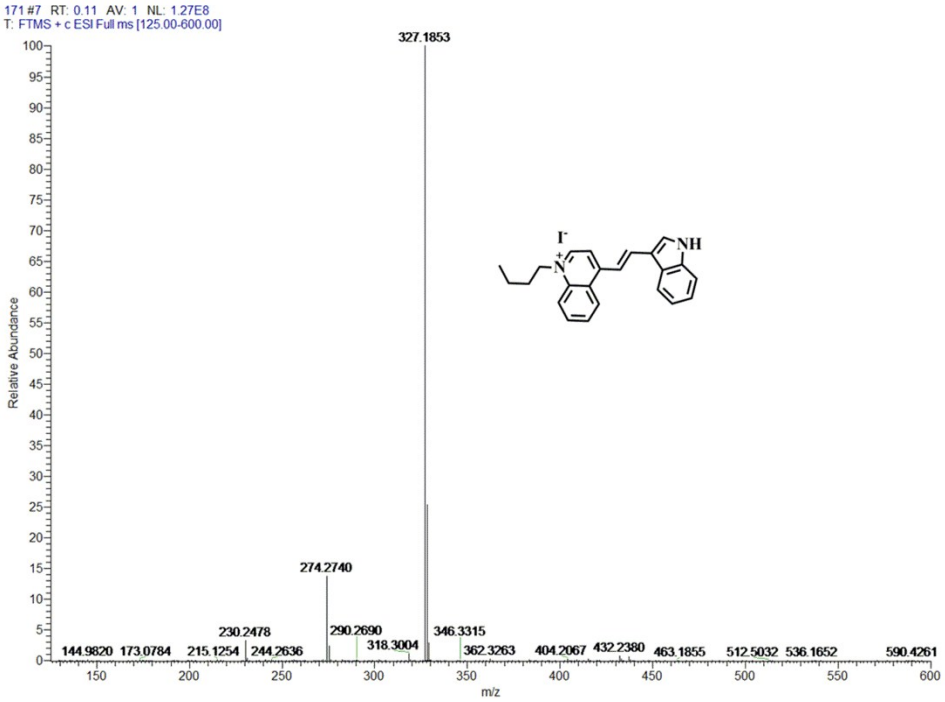

Figure. S2. MS Spectra of **IM-1**.

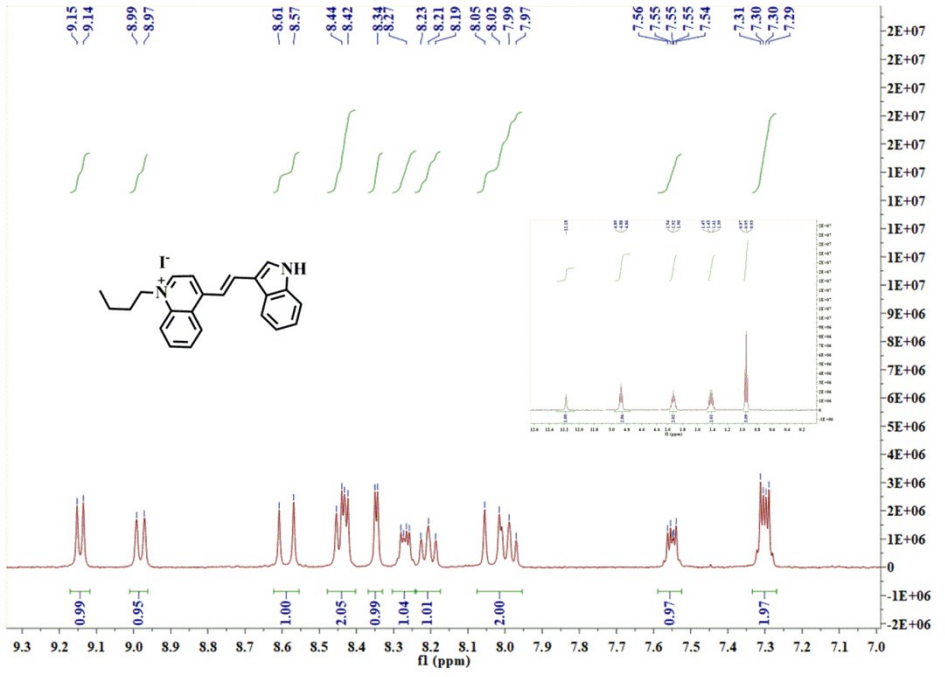

Figure. S3. [1]H NMR spectrum of **IM-1**.

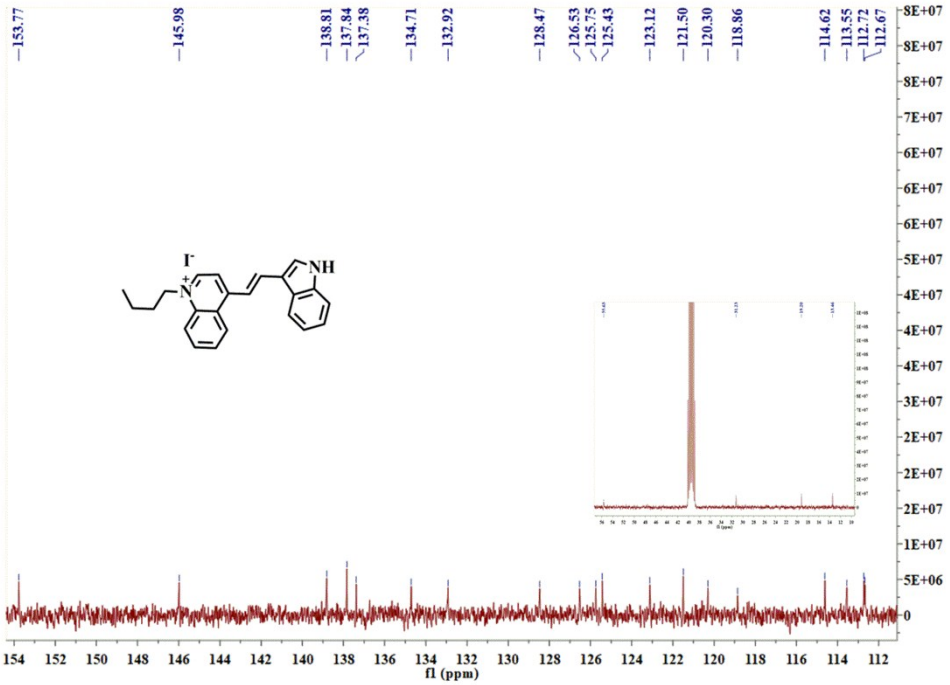

Figure. S4. ^{13}C NMR spectrum of **IM-1.**

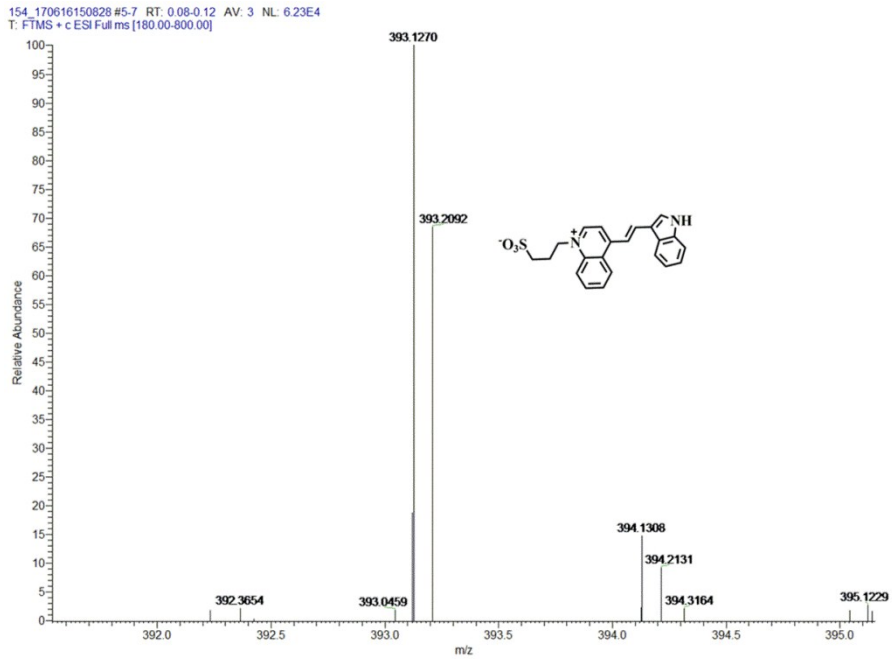

Figure. S5. MS Spectra of **IM-2.**

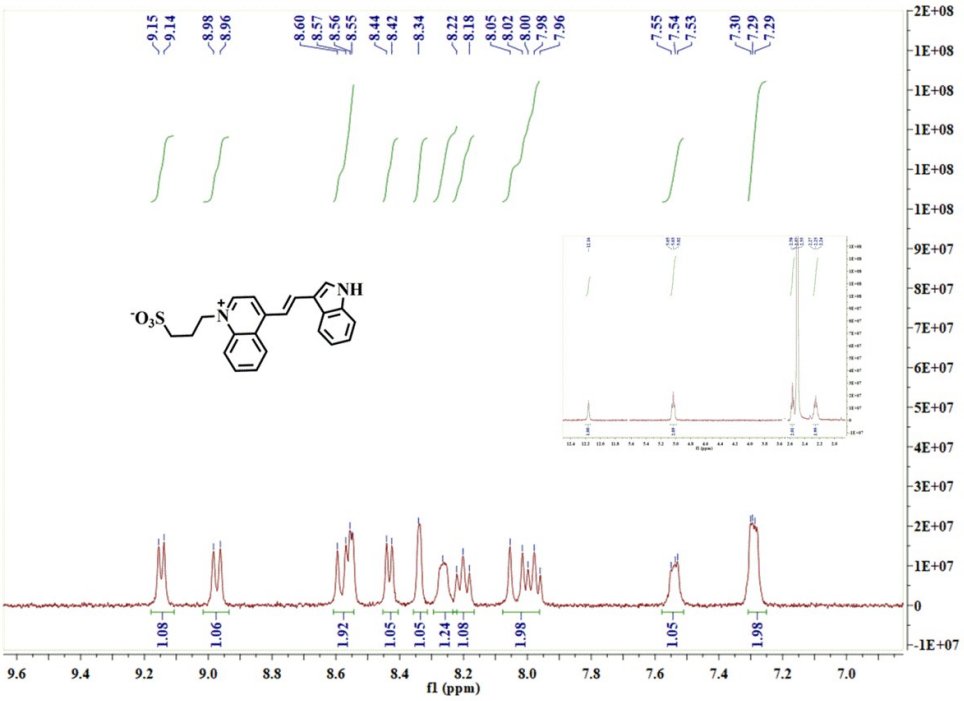

Figure. S6. ^{1}H NMR spectrum of **IM-2.**

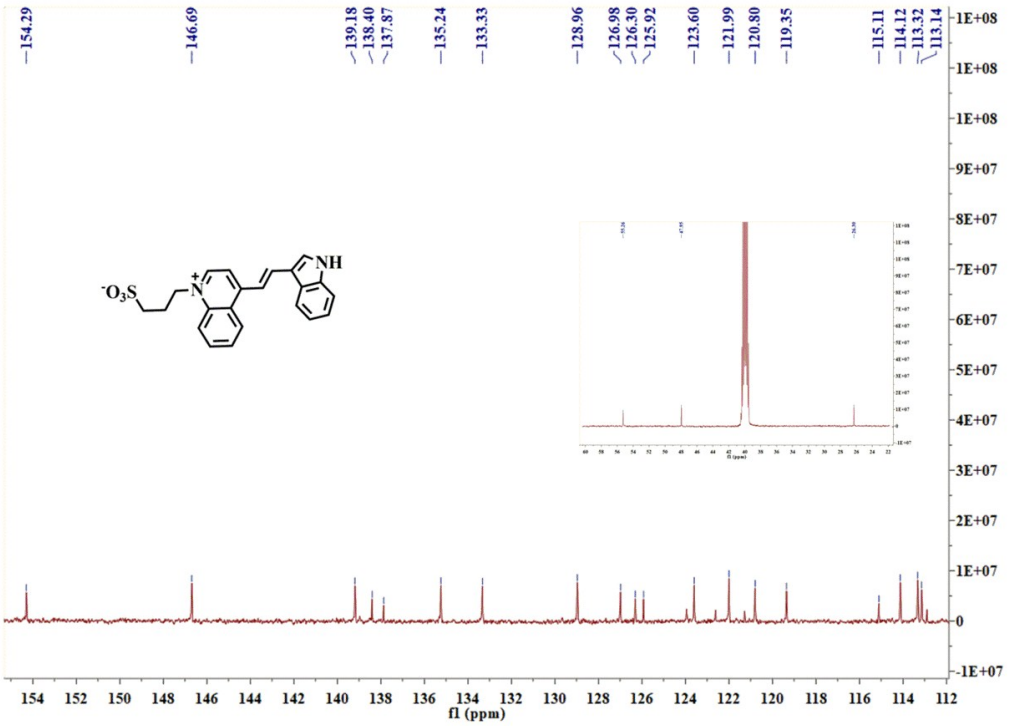

Figure. S7. ^{13}C NMR spectrum of **IM-2.**

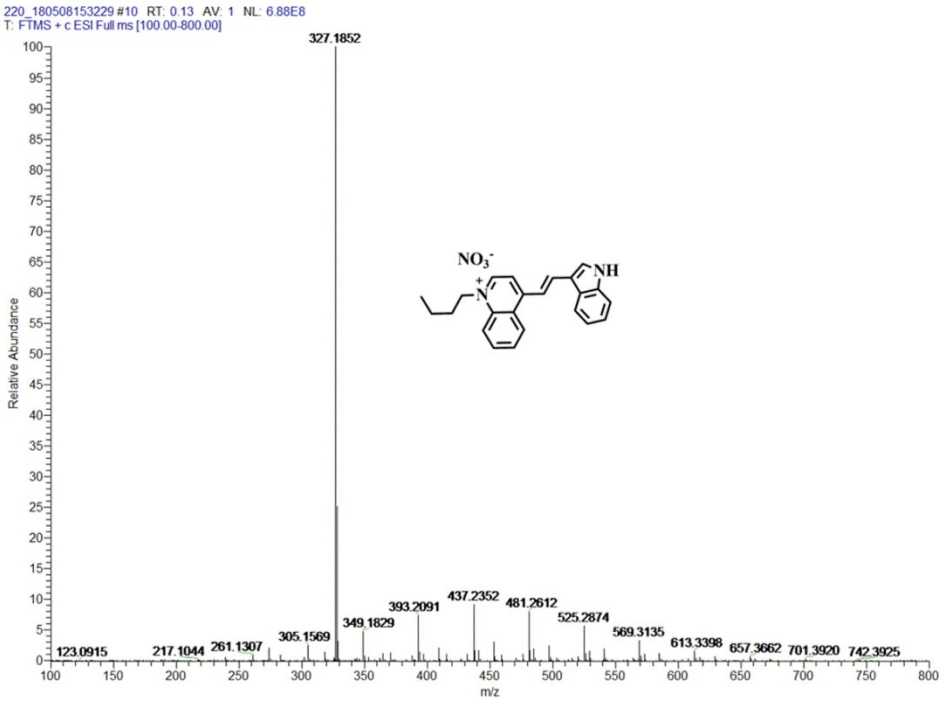

Figure. S8. MS Spectra of **IM-3.**

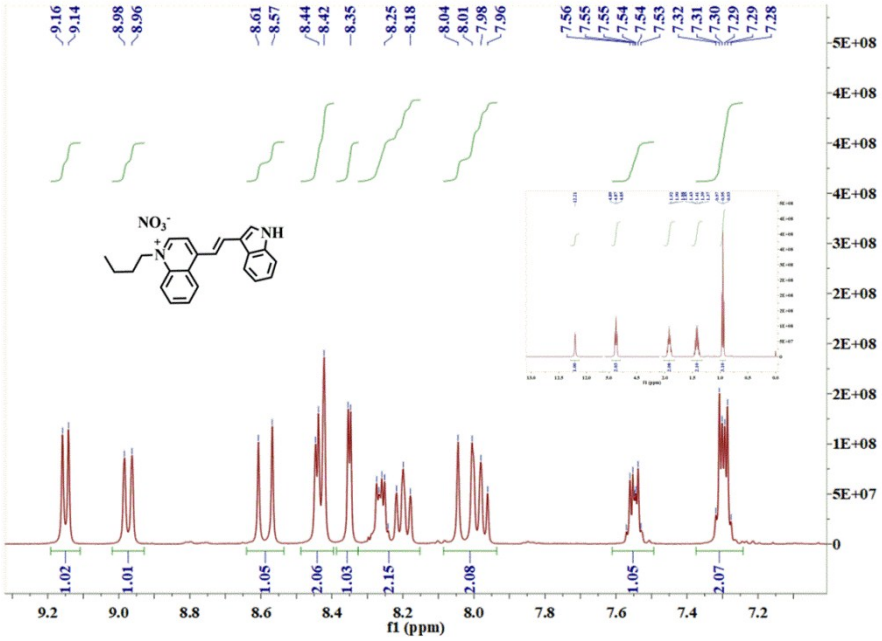

Figure. S9. ^{1}H NMR spectrum of **IM-3.**

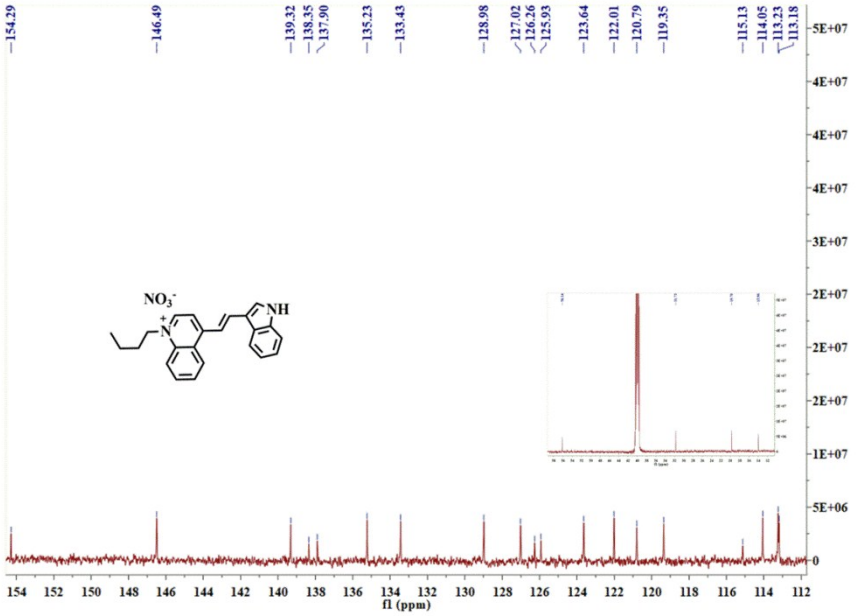

Figure. S10. ^{13}C NMR spectrum of **IM-3.**

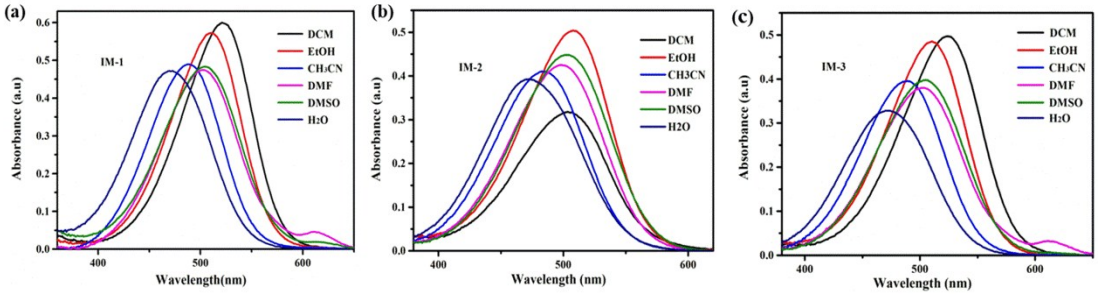

Figure. S11. Linear absorption spectra of **IM-1**, **IM-2** and **IM-3** in different solvents (c = 1.0 × 10^{-5} mol/L).

The UV-vis absorption and fluorescence spectra of all the compounds in different solvents are shown in (Fig.S11) and (Fig.S13) They display one absorption band at about 500 nm which is assigned to π - π* transitions[5]. The energy bands are further confirmed by TD-DFT calculations (Fig.S12) and (Table S5). For IM-3, the electron density of HOMO mainly focused on quinoline and indole rings, and mainly focused on quinoline ring at LUMO around 514 nm.

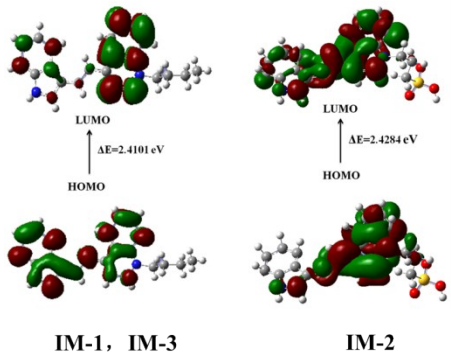

Figure. S12. Molecular orbital energy diagrams for **IM-1, IM-2** and **IM-3.**

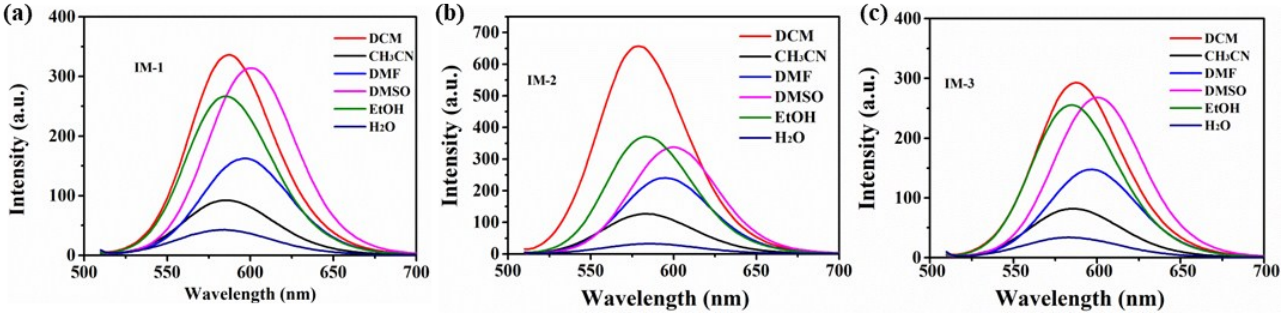

Figure. S13. Single-photon excited fluorescence spectra of **IM-1, IM-2** and **IM-3** in different solvents ($c = 1.0 \times 10^{-5}$ mol/L).

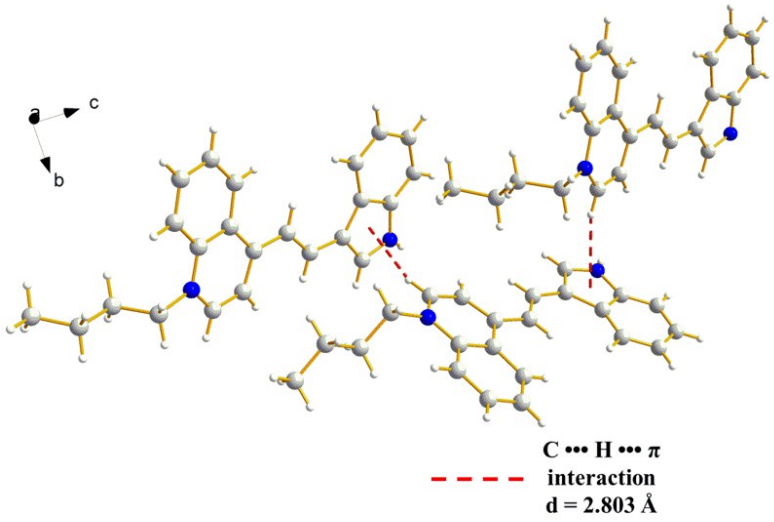

Figure. S14. The interactions in crystal structure of **IM-1.**

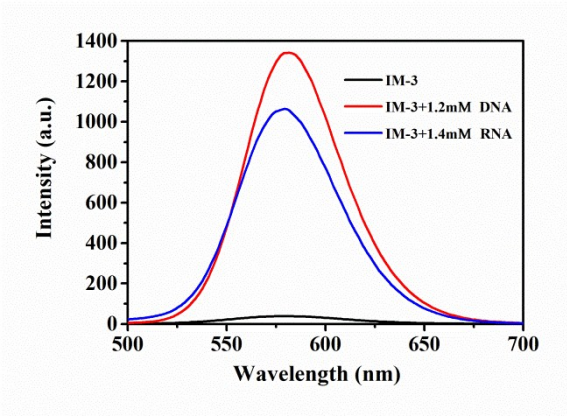

Figure. S15. The fluorescence enhancement of **IM-3** with DNA (1.2 mM) and RNA (1.4 mM).

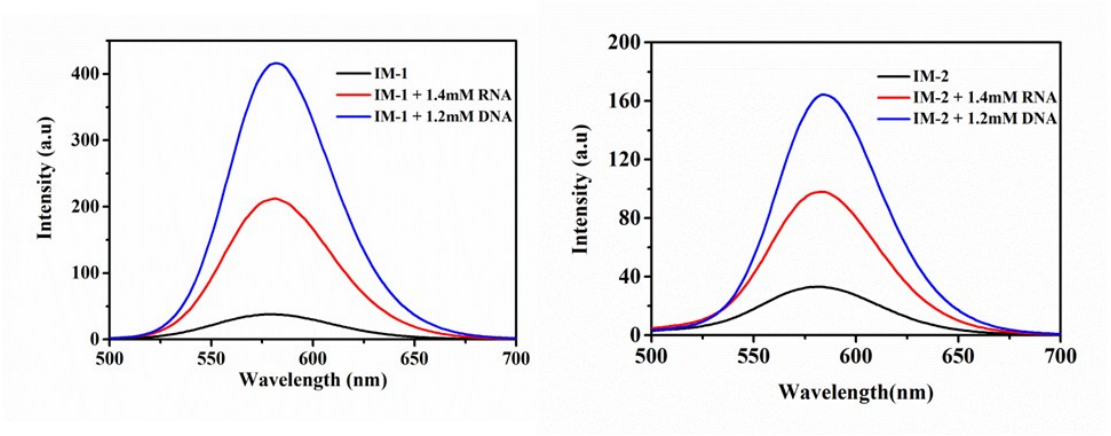

Figure. S16. The fluorescence enhancement of **IM-1** and **IM-2** with DNA (1.4 mM) and RNA (1.2 mM).

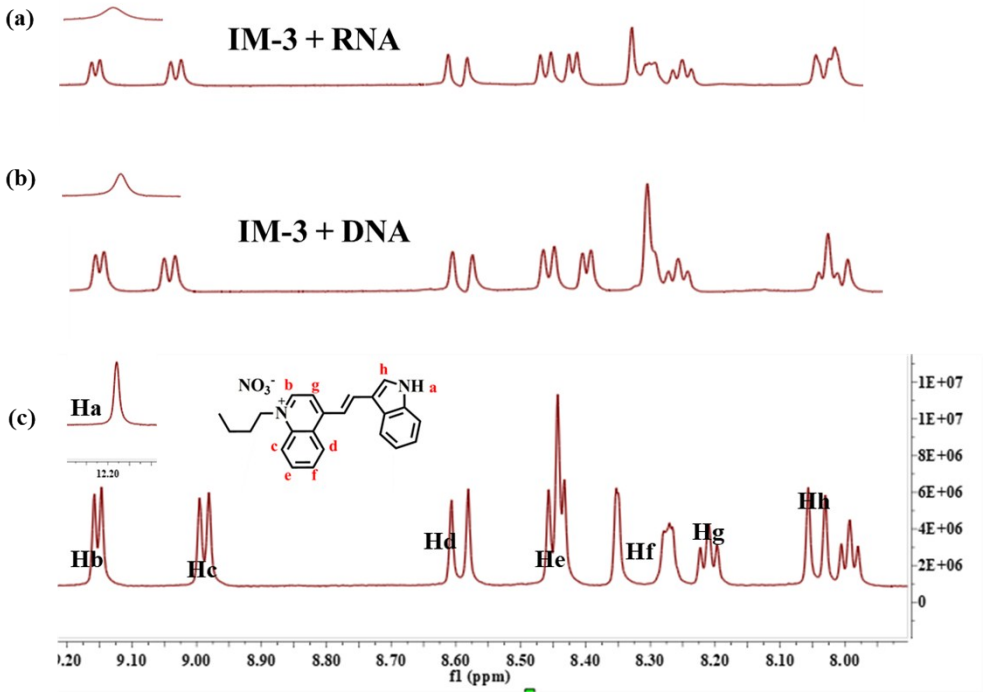

Fig S17 (a-b) STD NMR spectra of 1 mM IM-3 in the presence of 50 μM DNA/RNA. (c) Partial ^{1}H NMR spectra of IM-3 (1 mM) in DMSO-d_6/D_2O (v/v, 1:1)

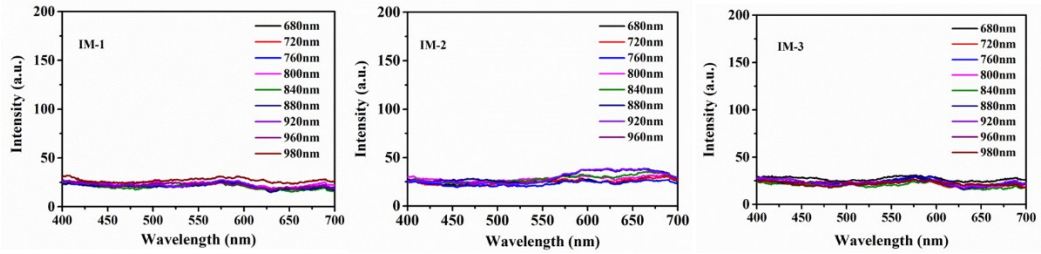

Figure. S18. Two-photon fluorescence spectra of **IM-1~IM-3** (1 mM) in water with different excitation wavelength.

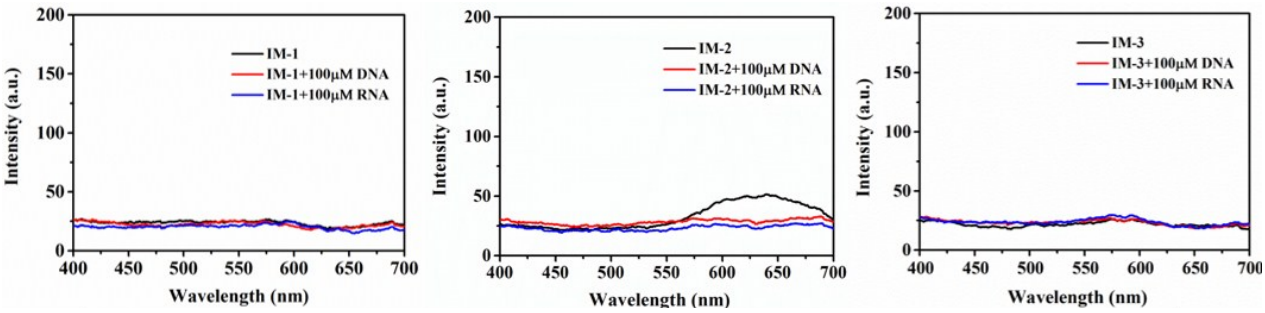

Figure. S19. The two-photon fluorescence spectra of **IM-1~IM-3** (1 mM) binding with 100 μM DNA/RNA under 880 nm excitation.

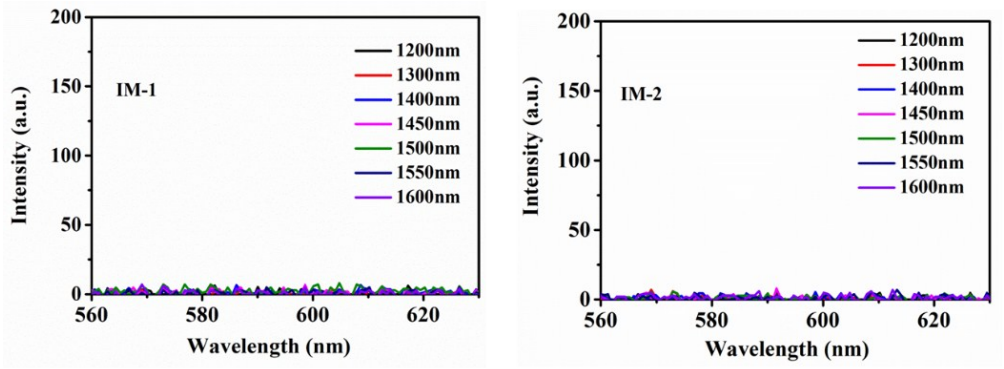

Figure. S20. Three-photon fluorescence spectra of **IM-1** and **IM-2** (1 mM) in water with different excitation wavelength.

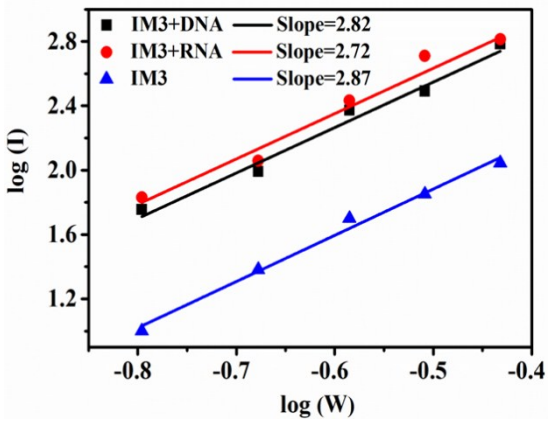

- **Figure. S21.** Three-photon verification of **IM-3** when 80 μM DNA/RNA was added.

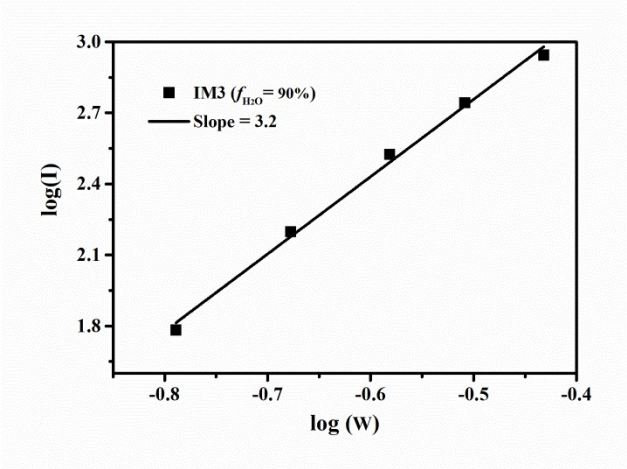

Figure. S22. Three-photon verification when **IM-3** (1 mM) in water/ ethanol (*f*w = 90 %).

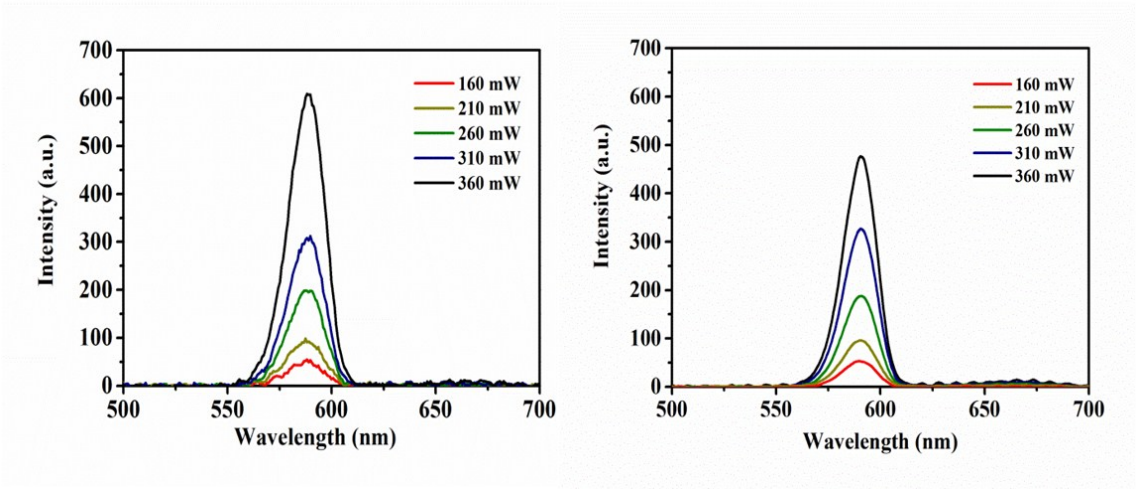

Figure. S23. Three-photon verification fluorescence of **IM-3** (1 mM) when 80 μM DNA/RNA was added.

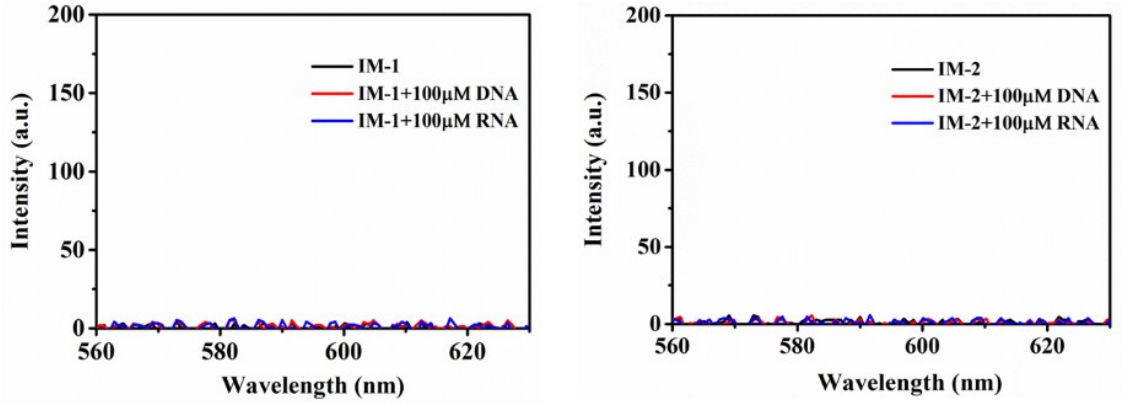

Figure. S24. The three-photon fluorescence spectra of **IM-1** and **IM-2** (1 mM) binding with 100 μM DNA/RNA under 1500 nm excitation.

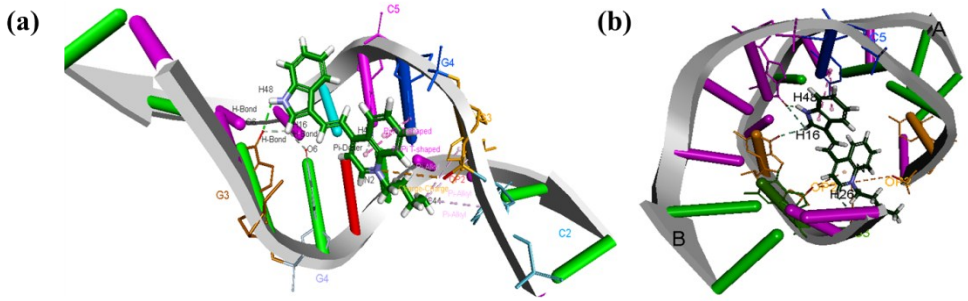

Figure. S25. Molecular modeling for the interaction of **IM-3** with DNA and RNA fragment.

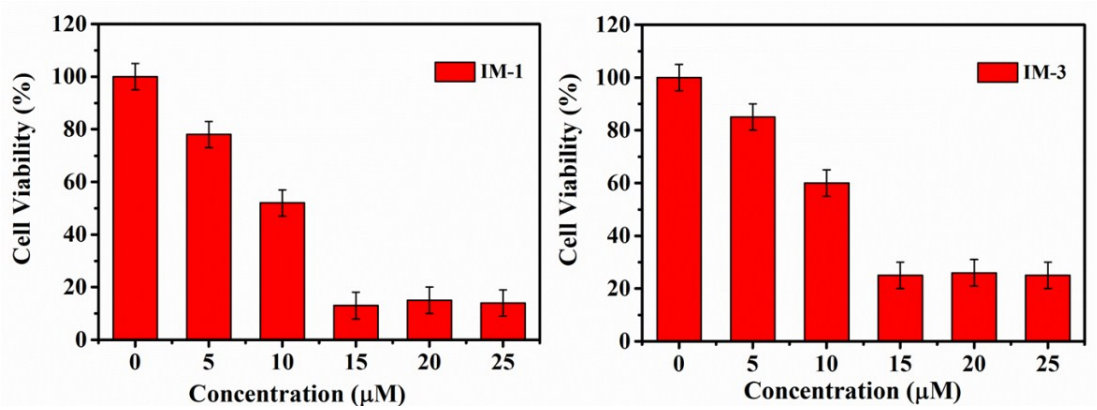

Figure. S26. Viability of HeLa cells in the presence of **IM-1** and **IM-3**.

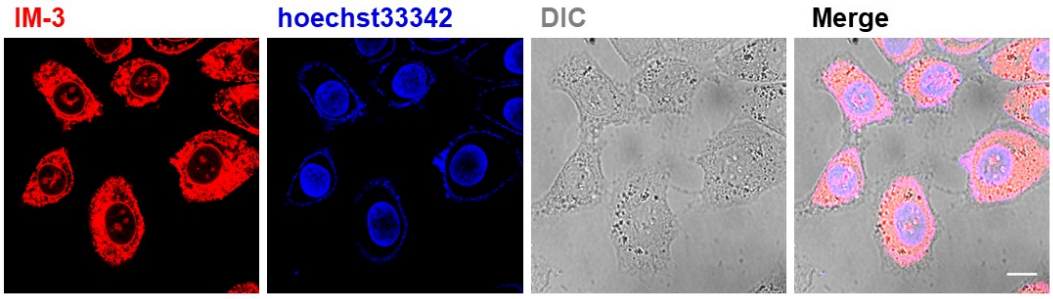

Figure. S27. Colocolization experiments using HepG2 cells incubated with **IM-3** (λ_{ex} = 405 nm, λ_{em} = 461 nm) and Hoechst 33342® (λ_{ex} = 346, λ_{em} = 460, scale bar = 5 μm)**.**

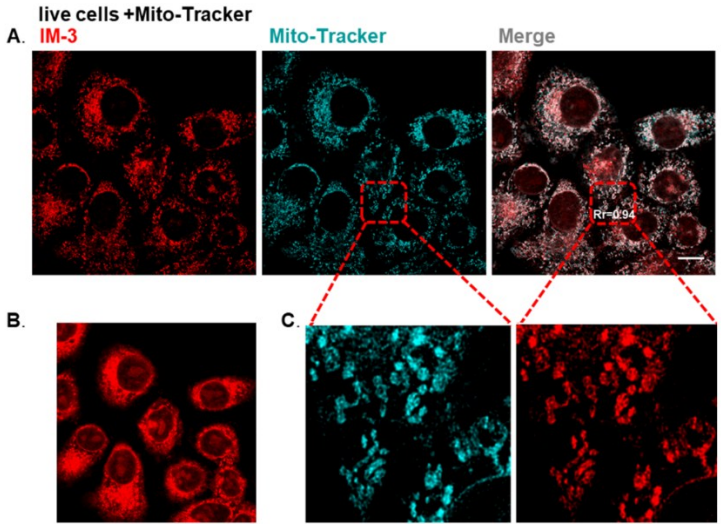

Figure. S28. (A) Colocolization experiments using Living HepG2 cells incubated with **IM-3** (λ_{ex} = 405 nm, λ_{em} = 461 nm) and Mito-Tracker deep red® (λ_{ex} = 633 nm, λ_{em} = 650 nm) (B) B is a diagram obtained by adjusting the Z-axis at the same position in Figure A to illustrate that **IM-3** can simultaneously label nucleoli and mitochondria (C) C is an enlargement of the area inside the dotted line of A (scale bar = 5 μm).

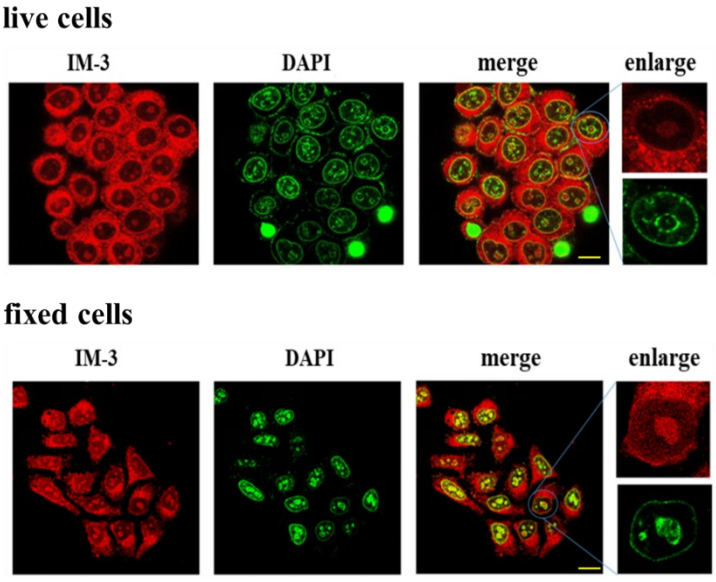

Figure. S29. IM-3 may simultaneously color RNA and cytoplasmic mitochondria in nuclear (λ_{ex}=405 nm, λ_{em}=461 nm, HepG2 cells, scale bar = 5 μm)**.**

Table S1. Crystal data collection and structure refinement of **IM-1** and **IM-2**.

Compound	IM-1	IM-2
Empirical formula	$C_{23}H_{23}IN_2$	$C_{22}H_{20}N_2O_3S$
Formula weight	454.33	392.12
T/K	296(2)	296.15
Crystal system, space group	Monoclinic, $P2_1/c$	Monoclinic, $P2_1/c$
Unit cell dimensions (Å,)	a=9.759(6) b=14.912(10) c=14.143(9) β=104.115(6)	a=10.532(2) b=13.748(3) c=14.154(3) β=92.091(2)
Volume/ $Å^3$	1996(2)	2048.0(7)
Z, Calculated density/Mg m^3	4, 1.512	4, 1.377
Absorption coefficient/mm^{-1}	1.613	0.192
F(000)	912.0	988.0
Goodness-of-fit on F^2	1.080	1.041
Final R indices [I>2σ]	R_1 = 0.0314, wR_2 = 0.0837	R_1 = 0.00422, wR_2 = 0.1087
Large diff. peak and hole/e $Å^{-3}$	0.34, -1.28	0.24, -0.48

Table S2. Selected bond lengths (Å) and angles (°) of IM-1 and IM-2.

IM-1			
N(1)-C(9)	1.383(4)	N(2)-C(15)	1.337(3)
N(1)-C(10)	1.337(4)	N(2)-C(5)	1.386(3)
C(20)-C(21)-C(22)	109.4(2)	C(10)-N(1)-C(9)	109.8(2)
C(2)-C(6)-C(7)	124.9(2)	C(15)-N(2)-C(5)	120.32(19)
IM-2			
S(1)-O(2)	1.450(4)	N(6)-C(22)	1.349(8)
S(1)-O(3)	1.447(4)	N(6)-C(21)	1.487(8)
O(3)-S(1)-O(2)	114.3(3)	O(3)-S(1)-C(12)	106.5(3)
C(22)-N(6)-C(10)	119.9(5)	C(24)-N(7)-C(23)	108.6(5)

- **Table S3 Log P value of IM-1, IM-2, IM-3**.

	Abs.	P	Log P
IM-1 in H_2O	2.03	2.20	0.34
IM-1 in Octanol	4.48		
IM-2 in H_2O	0.04	26.5	1.42
IM-2 in Octanol	1.06		
IM-3 in H_2O	2.37	1.80	0.25
IM-3 in Octanol	4.34		

Table S4. The photophysical data of **IM-1**, **IM-2** and **IM-3** in different solvents**.**

compound	Solvents	λ_{max}^{abs} (nm)[a]	λ_{max}^{SPEF} (nm)[b]	Δν(nm)[c]	Φ [d]
IM-1	DCM	521	587	66	
	Ethanol	509	584	78	
	Acetonitrile	487	583	96	
	DMF	502	597	95	
	DMSO	504	600	96	0.03
	Water	470	581	111	
IM-2	DCM	503	578	75	
	Ethanol	506	582	76	
	Acetonitrile	482	582	100	
	DMF	498	594	96	
	DMSO	502	600	98	0.04
	Water	471	583	112	
IM-3	DCM	525	588	63	
	Ethanol	509	585	76	
	Acetonitrile	487	586	99	
	DMF	501	597	96	
	DMSO	504	600	96	0.05
	Water	472	582	110	

[a] Peak position of the longest absorption band.

[b] Peak position of SPEF, excited at the absorption maximum.

[c] Stokes' shift in nm.

[d] Quantum yields determined by by using quinine sulfate as standard.

Table S5. Calculated linear absorption properties (nm), excitation energy (eV), oscillator strengths and major contribution for **IM-1**, **IM-2** and **IM-3**.

Cmpd	ΔE_1[a]	λ_{max}[nm][b]	Oscillator strengths	Nature of the transition
IM-1	2.410	514	0.0256	89(H)→90(L)(0.92962)
IM-2	2.428	510	0.0133	104(H)→105(L)(0.62179)
IM-3	2.410	514	0.0256	89(H)→90(L)(0.92962)

[a] The energy gap of the single-photon absorption band.

[b] Peak position of the maximum absorption band.

Table S6. The 3PA Cross-Section of **IM-3** in different ratios of ethanol and water with the excitation wavelength of 1600 nm.

	Excitation Wavelength (nm)	**3PA Cross-Section ($10^{-82}cm^6s^2photon^{-2}$)**
IM3 in ethanol	1600	1.46
IM3 in water/ethanol (*fw=5%*)	1600	4.11
IM3 in water/ethanol (*fw=50%*)	1600	7.03
IM3 in water/ethanol (*fw=70%*)	1600	6.03
IM3 in water/ethanol (*fw=90%*)	1600	24.21
IM3 in water	1600	36.02

Table S7. The 3PA Cross-Section of **IM-3** when different volume of DNA/RNA add with the excitation wavelength of 1500 nm**.**

	Excitation Wavelength (nm)	**3PA Cross-Section ($10^{-82}cm^6s^2photon^{-2}$)**
IM3(in PBS)	1500	25.64
IM3 + 20μM DNA	1500	64.04
IM3 + 40μM DNA	1500	81.07
IM3 + 60μM DNA	1500	84.19
IM3 + 80μM DNA	1500	103.60
IM3 + 100μM DNA	1500	76.47

IM3 + 20μM RNA	1500	62.83
IM3 + 40μM RNA	1500	93.86
IM3 + 60μM RNA	1500	103.01
IM3 + 80μM RNA	1500	123.19
IM3 + 100μM RNA	1500	97.29

References:

[1] S. V. Eliseeva, G. Aubock, F. V. Mourik, A. Cannizzo, B. Song, E. Deiters, A. S. Chauvin, M. Chergui and J. G. Bunzli, *J. Phys. Chem. B.*, 2010, **114**, 2932-2937.

[2] Z. H. Feng, D. D. Li, M. Z. Zhang, T. Shao, Y. Shen, X. H. Tian, Q. Zhang, S. L. Li, J. Y. Wu and Y. P. Tian, *Chem. Sci.,* 2019, **10**, 7228–7232.

[3] F. Shen, Z. Luo, H. Liu, R. Wang, S. Zhang, J. Gan, J. Sheng, *Nucleic Acids Res.*, 2017, **45**, 3537-3546.

[4] Dassault Systemes BIOVIA, Discovery Studio Modeling Environment, Release 2016, San Diego: Dassault Systems, 2016

[5] B. Fang, Y. Z. Zhu, L. Hu, Y. Shen, G. Q. Jiang, Q. Zhang, X. H. Tian, S. L. Li, H. P. Zhou, J. Y. Wu and Y. P. Tian, Inorg. chem., 2018, **57**, 14134-14143.